Abbreviations

%N	percentage nitrogen by mass
2-NDPA	2-Nitrodiphenylamine
AIMD	*ab initio* molecular dynamics
AO	atomic orbital
a.u.	atomic units
B3LYP	Becke, 3-parameter, Lee-Yang-Parr hybrid functional
BCP	bonding critical point
BSSE	basis set superposition error
CH_3CH_3	NC repeat unit with two $-OCH_3$ capping groups
CH_3OH	NC repeat unit with $-OCH_3$ capping group on ring 1 and $-OH$ group on ring 2
CCP	cage critical point
CP	critical point
DFT	density functional theory
DFT-D	density functional theory with dispersion correction
DSC	differential scanning calorimetry
DOS	degree of substitution
DPA	diphenylamine

EM energetic materials

EN ethyl nitrate

ESP electrostatic potential

G09 Gaussian 09 revision D.01

GGA generalised gradient approximation

GM genetically modified

GTO Gaussian type orbitals

GView Gauss View 5.0.8

HF Hartree-Fock

HMF hydroxymethylfurfural

HOMO highest occupied molecular orbital

IR infra-red spectroscopy

KS-DFT Kohn-Sham DFT

LDA local density approximation

MD molecular dynamics

MEP minimum energy path

MM molecular mechanics

MMFF94 Merck molecular force field 94

MO molecular orbitals

MP2 Møller–Plesset perturbation theory with second order correction

MW molecular weight

NBO natural bond orbital

NC nitrocellulose

NCP nuclear critical point

NG nitroglycerine

NMR nuclear magnetic resonance spectroscopy

$OHCH_3$ NC repeat unit with $-$OH capping group on ring 1 and $-OCH_3$ group on ring 2

PCM polarisable continuum model

PES potential energy surface

PETN pentaerythritol tetranitrate

PETRIN pentaerythritol trinitrate

QM quantum mechanics

QTAIM quantum theory of atoms in molecules

RCP ring critical point

RESP restrained electrostatic potential atomic partial charges

RHF restricted HF

ROHF restricted-open HF

UHF unrestricted HF

SB59 1,4-bis(ethylamino)-9,10-anthraquinone dye

SCF self-consistent field

SEM scanning electron microscopy

SMD solvation model based on density

S_N2 bi-molecular nucleophilic substitution reaction

STO Slater type orbitals

TG thermogravitmetric analysis

TS transition state

UFF universal force field

UV ultraviolet

UVvis ultraviolet–visible spectroscopy

vdW van der Waals

ωB97X-D ωB97X-D long-range corrected hybrid functional

ZPE zero-point energy

Chapter 1

Conclusion and future work

1.1 Conclusion

In this thesis, the degradation processes in nitrocellulose (NC) were explored using computational methods to elucidate the dominant processes and key reactants involved in ambient ageing. In the first section, the polymeric structure of NC was introduced. Different sized truncations were tested as approximations for the polysaccharide. This was achieved by inspection of the partial charges, electrostatic potential (ESP) and critical interaction points for monomeric, dimeric and trimeric β-glucopyranose structures. The dimer was found to be the minimum structure required to reproduce the full properties of NC within a repeat unit. As a result of the high degrees of freedom and flexibility of the larger structures, the monomeric structure was instead chosen for subsequent mechanistic studies, to speed up geometry optimisation and simplify already challenging transition state (TS) searches.

Methoxy and hydroxyl capping groups were compared; the methoxy groups provided a more sterically and chemically similar proxy for the extended polymer, following examination of charges and geometry dependent interactions. Comparison of the charge densities and intramolecular interactions around the monomer and dimer revealed that the former exhibited an acceptable level of deviation from the dimer behaviour , particularly with reference to further investigations concentrating only on localised reaction interactions. The bi-methoxy monomer was implemented as the model for NC in later studies.

Using the monomer model, the primary steps of decomposition were explored in Chapter **??**. Thermolytic denitration reactions were investigated; homolytic fission of the nitrate $O-NO_2$ bond, and elimination of HNO_2 were tested for both the PETN test case, and the NC monomer model. Good agreement with literature values was found for the reaction energies and activation energies, in case of HNO_2 elimination in both pentaerythritol

tetranitrate (PETN) and NC. The loss of $^{\cdot}NO_2$ *via* homolysis was confirmed. For the acid hydrolysis pathway , possible protonation sites in the monomer were analysed. It was found that the proton site most amenable to denitration was the bridging oxygen position of the nitrate. Further investigations considered denitration routes beginning from isomers protonated at both the terminal (upper) and bridging sites. The denitration step was then explored *via* a series of potential energy surface (PES) scans. The stability of different possible TS ring structures involving both pre-protonation and concerted protonation-denitration was examined, in addition to the nature of the NO_2 leaving group. No stable TS structures presenting the correct vibration for denitration were isolated, however scans confirmed that the NO_2 was released as NO_2^+, with possible formation of HNO_2 at greater separations.

Proposed decomposition routes originating from the primary denitration step were collated from nitrate ester reactions in literature. Using ethyl nitrate (EN) as an initial test case, the energies of each reaction were evaluated to determine whether it were a viable secondary reaction step following liberation of the $^{\cdot}NO_2$, NO_2^+ or HNO_2 following first stage decomposition. Possible decomposition schemes were constructed, mapping from the point of NO_2 liberation to the oxidation of the alcohol group. The reaction energies were determined for the NC monomer. It was found that the energies were largely favourable from a thermodynamic equilibrium perspective. The fate of the released nitrogen species was in the accumulation of N_2O or regeneration of $^{\cdot}NO_2$, suggesting $^{\cdot}NO_2$ as the species responsible for autocatalytic processes in the system. Consumption of $^{\cdot}NO_2$ in the formation of acids proved to be thermodynamically unfavourable.HNO_2 routes lead to the formation of N_2O without self-regeneration and HNO_3 routes lead primarily to formation of $^{\cdot}NO_2$. This indicates that HNO_2 was unlikely to be a direct contributor to catalysis, and that HNO_3 was the precursor to the $^{\cdot}NO_2$ catalytic species, acknowledging experimental observations that HNO_3 appared to facilitate autocatalysis [1].

Whilst this work has not exhaustively explored the myriad reactions that may occur in the complex ageing procedures of NC, it has established the key reactions of the early stages of degradation, with presentation of an effective truncation of the polymeric structure applicable for further study in the topic. Key competing reactions for the denitration step, the identity of nitrogen species released and their role in the longer-range decomposition process has been presented. The conclusion of this project sets the scope for subsequent investigations into the later-stage reaction processes that lead to deeper degradation of the

NC backbone.

1.2 Further Work

For the refinement the existing NC model, a more rigorous examination of the partial charges and the subtle variation in geometry, may be conducted. This includes explicit calculation of charges, perhaps using NBO methods [2, 3] or RESP charges [**?**, 4], as has been applied to other saccharide and hetercyclic organic compounds. Conformational scans, in particular for the C6 chain, and for the orientation of the units within the trimer, would be beneficial for identification of other low energy structures likely to be present in the natural polymer. Here, only the denitration schemes for the singly nitrated NC monomer were documented. The differing stabilities of NC at varying levels of nitration will undoubtedly affect the reactivity at each site. Propagation of different nitration level and conformational structures through the denitration and secondary decomposition schemes may reveal alternative reactions, or alter the balance of products obtained.

Classical molecular dynamics (MD) techniques would also provide further insight into the diffusion of the released products, and their interaction with the wider polymer. Studies involving the interaction of NC with plasticisers has effectively probed the diffusion rates of plasticiser migration, which is of key interest in the preservation of stable NC product formulations [5].

Another avenue of interest is in the exploration of other transition structures for the denitration stage, and for further degradation following formation of the ketone. The inclusion of additional explicit water molecules or water clusters may stabilise TS that were previously not viable, starting with reproduction of those for **Momany2005!** (**Momany2005!**). AIMD techniques may be effective for the elucidation of water and acid interactions with NC, probing protonation behaviour and water clustering around monomer, dimer and trimer structures at different degree of substitution (DOS) [6].

A natural extension to the study of the secondary reactions driving decomposition, is the expansion to a wider range of possible reaction pathways. These may include the widely documented mechanisms studied for glucose (figure 1.1) **Qian2009,Qian2010,Qian2011!** (**Qian2009,Qian2010,Qian2011!**). This is in addition to further studies of possible ring opening mechanisms and chain scission reactions, in order to fully account for the broad spectrum of experimentally observed degradation products in infra-red spectroscopy (IR) and nuclear magnetic resonance spectroscopy (NMR) measurements [8, 9, 10, 11, 12, 13].

(a) Conversion of glucose A to hydroxymethylfurfural (HMF) C *via* a furan aldehyde intermediate B.

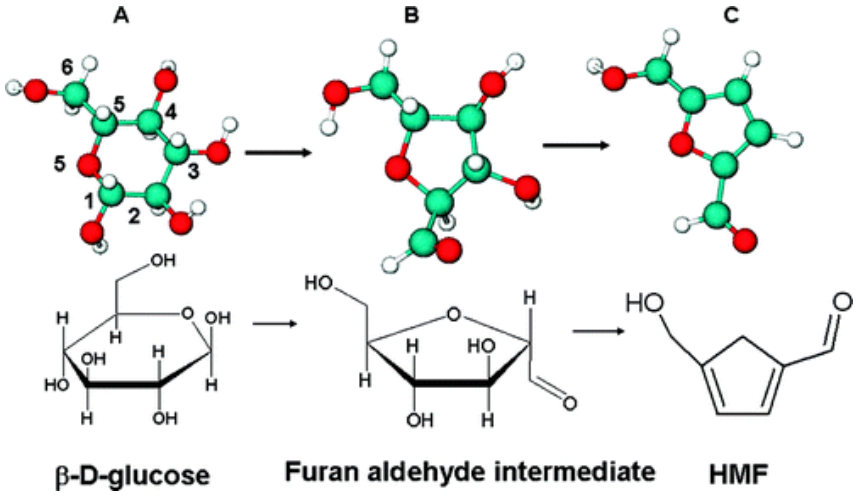

(b) CV3: Protonation of C2–OH on β-d-glucose, CV2: subsequent breakage of the C_2-O_2 Bond, CV1: the formation of the C2–O5 bond during glucose conversion to HMF.

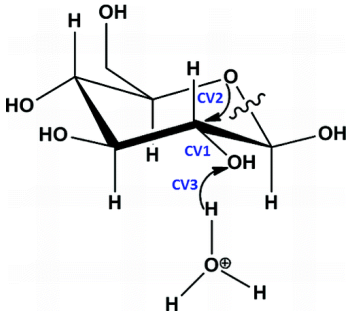

Figure 1.1: The conversion of glucose to HMF with 1.1a) showing the proposed reaction scheme, and 1.1b) displaying a possible mechanistic pathway, from the *ab initio* molecular dynamics (AIMD) study by Qian [7].

Bibliography

[1] John W. Baker and D. M. Easty. Hydrolytic decomposition of esters of nitric acid. Part I. General experimental techniques. Alkaline hydrolysis and neutral solvolysis of methyl, ethyl, isopropyl, and tert.-butyl nitrates in aqueous alcohol. *Journal of the Chemical Society (Resumed)*, 1952(0):1193–1207, 1952.

[2] Hong Bin Xie, Lin Jin, Svemir Rudić, John P. Simons, and R. Benny Gerber. Computational studies of protonated β-d-galactose and its hydrated complex: Structures, interactions, proton transfer dynamics, and spectroscopy. *Journal of Physical Chemistry B*, 116(16):4851–4859, 2012.

[3] David Santos-Carballal, Reynier Suardíaz, Rachel Crespo-Otero, Leandro González, and Carlos S. Pérez. Conformational and NMR study of some furan derivatives by DFT methods. In *Journal of Molecular Modeling*, volume 19, pages 4591–4601. Springer Berlin Heidelberg, oct 2013.

[4] R.J Woods and R Chappelle. Restrained electrostatic potential atomic partial charges for condensed-phase simulations of carbohydrates. *Journal of Molecular Structure: THEOCHEM*, 527(1-3):149–156, aug 2000.

[5] Lisa A. Richards, Anthony Nash, Maximillian Joshua Sebastian Phipps, and Nora H. De Leeuw. A molecular dynamics study of plasticiser migration in nitrocellulose binders. *New Journal of Chemistry*, 42(21):17420–17428, oct 2018.

[6] Diego Ardura and D. J. Donaldson. Where does acid hydrolysis take place? *Phys. Chem. Chem. Phys.*, 11(5):857–863, feb 2009.

[7] Xianghong Qian. Mechanisms and energetics for acid catalyzed β-D-glucose conversion to 5-hydroxymethylfurfurl. *Journal of Physical Chemistry A*, 115(42):11740–11748, 2011.

[8] Yulia A. Gismatulina, Vera V. Budaeva, and Gennady V. Sakovich. Nitrocellulose Synthesis from Miscanthus Cellulose. *Propellants, Explosives, Pyrotechnics*, 43(1):96–100, jan 2018.

[9] V. I. Kovalenko, R. M. Mukhamadeeva, L. N. Maklakova, and N. G. Gustova. Interpretation of the IR spectrum and structure of cellulose nitrate. *Journal of Structural Chemistry*, 34(4):540–547, 1994.

[10] Liu Huwei and Fu Ruonong. Studies on thermal decomposition of nitrocellulose by pyrolysis-gas chromatography. *Journal of Analytical and Applied Pyrolysis*, 14(2-3):163–169, dec 1988.

[11] L. Dauerman and Y. A. Tajima. Thermal decomposition and combustion of nitrocellulose. *AIAA Journal*, 6(8):1468–1473, aug 1968.

[12] D.T. Clark and P.J. Stephenson. A 13C n.m.r. and X-ray study of the relationship between the distribution of nitrate ester groups and interchain d(110) spacings in a series of cellulose nitrates. *Polymer*, 23(9):1295–1299, aug 1982.

[13] Ting Kai Wu. Carbon-13 and Proton Nuclear Magnetic Resonance Studies of Cellulose Nitrates. *Macromolecules*, 13(1):74–79, jan 1980.